

Multiwavelength Modeling Results of Two States of the Distant HBL 1ES 0647+250

1ES 0647+250 is a seemingly distant very-high-energy (VHE; >0.1 TeV) emitting blazar, classified as a high-frequency-peaked BL Lac (HBL) [1]. In 2011, 1ES 0647+250 was discovered in VHE by MAGIC [2]. There is no spectroscopic redshift measurement but an imaging redshift of $z=0.45$ ($+0.11$, -0.10) was derived assuming the host galaxy is a standard candle [3]. According to TeVCat, adopting a redshift of $z=0.45$ would place 1ES 0647+250 among the most distant HBLs observed at VHE energies. Our goal is to understand the physical emission mechanisms dominant in 1ES 0647+250. We do this by modeling two steady-state multiwavelength spectral energy distributions (SEDs) with multiwavelength coverage—a high flux state in 2020 and a low flux state in 2012.

We model a high flux state and a low flux state. The high (low) state is the highest (lowest) state observed by the Very Energetic Radiation Imaging Telescope Array System (VERITAS) with sufficient multiwavelength coverage. The **high state** spans from 2020 Dec 17 to 22 (inclusive). The **low state** covers 2012 December 8 to Dec 21 (inclusive), and the *Fermi*-LAT data span a longer period from 2012 Nov 17 to 2013 Jan 12 to obtain sufficient statistics.

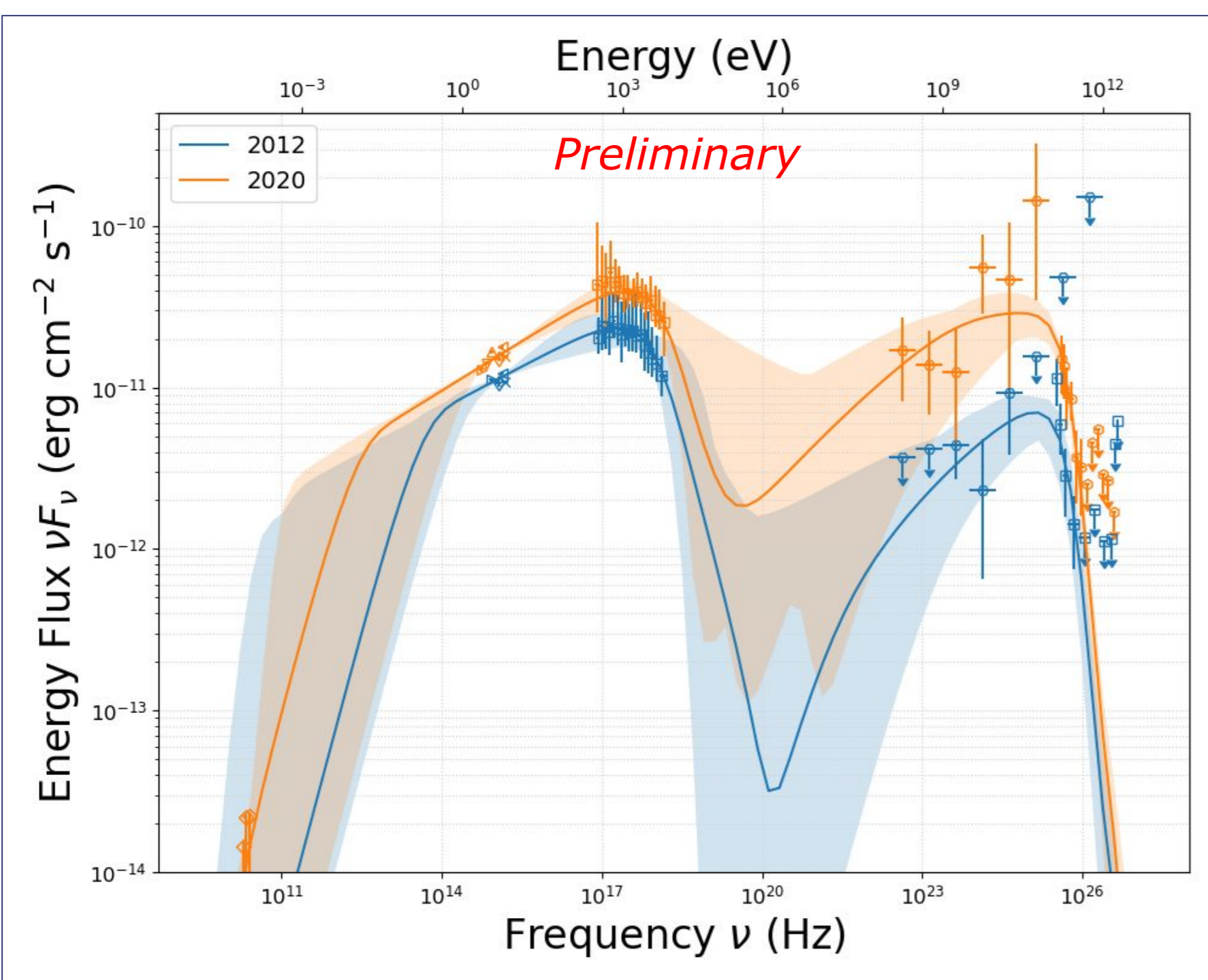


Figure 1: SED resulting from a synchrotron self-Compton fit to two states: (orange) high state in December 2020 and (blue) low state in December 2012. The 1σ contour is associated with the parameter uncertainties. Two unconstraining upper limits from *Fermi*-LAT are not shown.

Differences in the models

The spectral energy distributions (SEDs) of the high state and low state are in Figure 1, as well as the fit to a synchrotron self-Compton (SSC) model. The high state has a higher flux at all frequencies. As can be seen in Figure 1 and Table 1, during the high state the synchrotron peak frequency is higher and the inverse Compton peak frequency is lower. As shown in Figures 2 and 3, the most dramatic parameter changes between the two states are the minimum Lorentz factor of the electrons γ_{\min} , electron index before the break n_1 , and magnetic field strength B . Comparing the high state and low state, the minimum Lorentz factor of the electrons γ_{\min} has a statistical difference of 2.5σ ; no other parameters have a statistical difference above 2σ . Also shown in Figures 2 and 3 is that the electron index after the break n_2 is similar between the low state and high state.

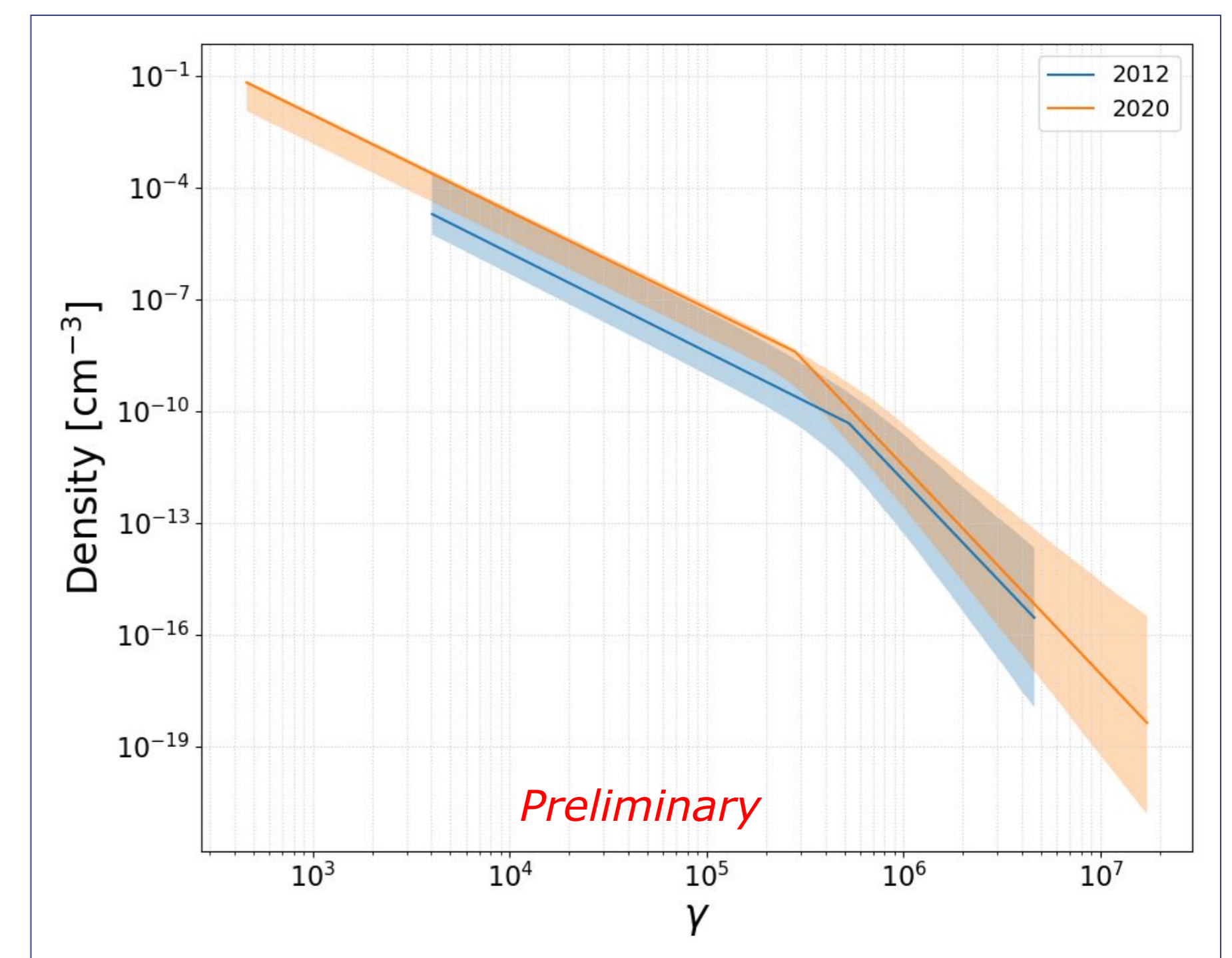


Figure 2: Electron distribution (Equation 1) from a synchrotron self-Compton fit to two states: (orange) high state and (blue) low state. The 1σ contour is associated with the parameter uncertainties, excluding the uncertainties on γ_{\min} and γ_{\max} .

	Flux >0.15 TeV [$\text{ph}/\text{m}^2/\text{TeV}/\text{s}$]	Flux >0.15 TeV [% Crab]	VHE power law index	Reduced chi-squared of SSC fit	Synchrotron peak [Hz]	Inverse Compton peak [Hz]
High State (2020)	$(20.5 \pm 3.3) \times 10^{-8}$	5.9 ± 0.9	4.4 ± 0.7	$48.45/36=1.35$	3.1×10^{17}	5.9×10^{24}
Low State (2012)	$(7.6 \pm 1.8) \times 10^{-8}$	2.2 ± 0.5	5.0 ± 0.9	$24.39/30=0.81$	2.0×10^{17}	1.5×10^{25}

Table 1: Comparison of properties of two states. The VHE emission displays harder-when-brighter behavior. The synchrotron peak is consistent with the HBL classification. The estimates of the synchrotron and inverse Compton peak frequencies do not consider the contours.

$$N_e(\gamma) = \begin{cases} K\gamma^{-n_1} & \gamma_{\min} \leq \gamma \leq \gamma_{\text{break}} \\ K\gamma_{\text{break}}^{n_2-n_1}\gamma^{-n_2} & \gamma_{\text{break}} \leq \gamma \leq \gamma_{\max} \end{cases}$$

Equation 1: Broken power law which describes the electron distribution in the synchrotron self-Compton emission zone in the Bjet_MCMC framework. Note that $K=N_e(1)$.

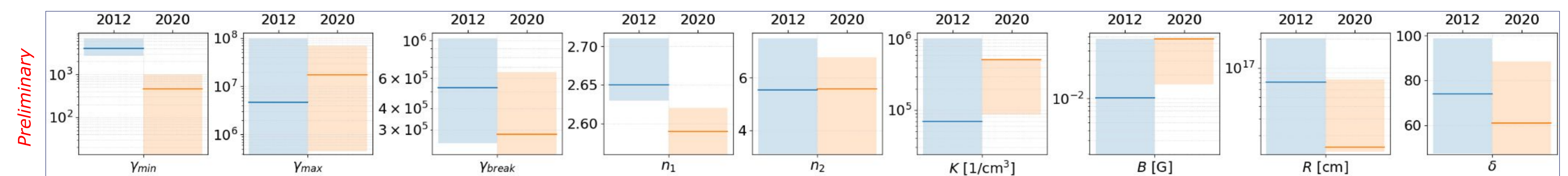


Figure 3: Parameters from a synchrotron self-Compton fit to two states: (orange) high state and (blue) low state. Parameters γ_{\min} to K correspond to Equation 1. In addition, the model is classified by the blob magnetic field B , the blob size R , and the blob Doppler factor δ . The solid line represents the best fit. The shaded bars represent the 1σ parameter bounds.

Methods

Which data?

Data was analysed or obtained from the TeV Effelsberg Long-term AGN Monitoring (TELAMON) [4, 5], *Swift* Ultraviolet/Optical Telescope (UVOT) [6], *Swift* X-Ray Telescope (XRT) [7], *Fermi* Large Area Telescope (LAT) [8], and the Very Energetic Radiation Imaging Telescope Array System (VERITAS) [9]. Contemporaneous data sets with sufficient statistics and multiwavelength coverage were identified. The low state and high state were identified using high-energy and very-high-energy light curves from *Fermi*-LAT and VERITAS. The precise dates are

- 2012 December 8 to Dec 21 (inclusive), with *Fermi*-LAT data which span 2012 Nov 17 to 2013 Jan 12, and
- 2020 Dec 17 to Dec 22 (inclusive).

Which model?

Because 1ES 0647+250 is an HBL, its high energy emission is likely due to synchrotron self-Compton (SSC) emission [10]. Thus, a SSC model was applied to 1ES 0647+250. In the leptonic, synchrotron self-Compton framework, the same population of electrons produce synchrotron radiation and inverse Compton emission. Bjet_MCMC [11] was used to apply a one-zone SSC model. In Bjet_MCMC (or “blob-in-jet” MCMC), the emission from a “blob” is considered. The blob is a compact, spherical, high-energy emission zone with an isotropic distribution of electrons and a magnetic field of constant magnitude and tangled direction. The electrons are distributed according to a broken power law (Equation 1).

Which model inputs?

The model depends on several user-set parameters:

- Redshift. A photometric redshift places 1ES 0647+250 at $z=0.45$ ($+0.11$, -0.10) [3].
- Fastest observed variability. This was determined from the fastest flux doubling time of the X-ray light curves. The result is 35 hours for 2012, and 69 hours for 2020.

The defaults are used for the remaining parameters:

- Cosmology: $H_0=69.6$ km/s/Mpc, $\Omega_M=0.286$, and $\Omega_\Lambda=0.714$ [12].
- Viewing angle: $\theta=0.57^\circ$. At the time of writing, no information about the viewing angle of 1ES 0647+250 exists in the literature, so the default viewing angle is used, compatible with $\delta \sin \theta < 1$ and $\delta \leq 100$.

References

- [1] Costamante & Ghisellini. 2002. A&A, 384, p56.
 [2] Barbara De Lotto and the MAGIC Collaboration 2012 J. Phys.: Conf. Ser. 375 052021
 [3] Meisner & Romani. 2010, ApJ, 712, p14.
 [4] https://telamon.astro.uni-wuerzburg.de
 [5] Eppel et al. 2024, A&A, 684, A11
 [6] https://swift.gsfc.nasa.gov/about_swift/uvot_desc.html
 [7] https://swift.gsfc.nasa.gov/about_swift/xrt_desc.html
 [8] https://fermi.gsfc.nasa.gov
 [9] https://veritas.sao.arizona.edu

Acknowledgments

This research is supported by grants from the U.S. DoE, the NSF, and the Smithsonian, by NSERC in Canada, and by the Helmholtz Association in Germany. We also gratefully acknowledge the excellent work of our technical support staff. The TELAMON program is using the Effelsberg 100-m telescope to monitor the radio spectra of active galactic nuclei (AGN) under scrutiny in astroparticle physics, namely TeV blazars and candidate neutrino-associated AGN. We thank the TELAMON Collaboration for providing data.

Megan Spletstoesser¹ (she/her) for the VERITAS² Collaboration

¹University of California, Santa Cruz ²https://veritas.sao.arizona.edu

8th Heidelberg International Symposium on High-Energy Gamma-Ray Astronomy (γ -2024)



UC SANTA CRUZ